

General Disclaimer

One or more of the Following Statements may affect this Document

- This document has been reproduced from the best copy furnished by the organizational source. It is being released in the interest of making available as much information as possible.
- This document may contain data, which exceeds the sheet parameters. It was furnished in this condition by the organizational source and is the best copy available.
- This document may contain tone-on-tone or color graphs, charts and/or pictures, which have been reproduced in black and white.
- This document is paginated as submitted by the original source.
- Portions of this document are not fully legible due to the historical nature of some of the material. However, it is the best reproduction available from the original submission.

(NASA-TM-X-73196) COMMENT ON THE RELATION
BETWEEN THE NONADIABATIC COUPLING AND THE
COMPLEX INTERSECTION OF POTENTIAL ENERGY
CURVES (NASA) 20 p HC A02/MF A01 CSCL 20H

N77-15809

Unclas
G3/72 11537

**NASA TECHNICAL
MEMORANDUM**

NASA TM X-73,196

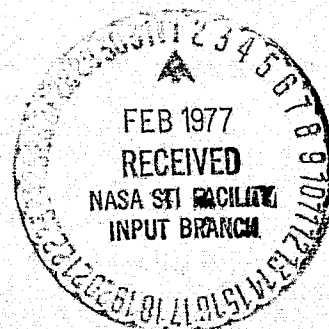
NASA TM X-73,196

**COMMENT ON THE RELATION BETWEEN THE NONADIABATIC
COUPLING AND THE COMPLEX INTERSECTION OF POTENTIAL
ENERGY CURVES**

Richard L. Jaffe

**Ames Research Center
Moffett Field, Calif. 94035**

January 1977



1. Report No. NASA TM X-73,196		2. Government Accession No.		3. Recipient's Catalog No.	
4. Title and Subtitle COMMENT ON THE RELATION BETWEEN THE NONADIABATIC COUPLING AND THE COMPLEX INTERSECTION OF POTENTIAL ENERGY CURVES				5. Report Date	
				6. Performing Organization Code	
7. Author(s) Richard L. Jaffe*				8. Performing Organization Report No. A-6705	
9. Performing Organization Name and Address Ames Research Center, NASA Moffett Field, Calif. 94035				10. Work Unit No. 506-16-12	
				11. Contract or Grant No.	
12. Sponsoring Agency Name and Address National Aeronautics and Space Administration Washington, D.C. 20546				13. Type of Report and Period Covered Technical Memorandum	
				14. Sponsoring Agency Code	
15. Supplementary Notes *NASA/NRC Research Associate, 1974-1976.					
16. Abstract Simple relations are discussed that provide a correspondence between the complex intersection of two potential surfaces and the nonadiabatic coupling matrix element between those surfaces. These are key quantities in semiclassical and quantum mechanical theories of collision-induced electronic transitions. Within the two-state approximation, the complex intersection is shown to be directly related to the location and magnitude of the peak in the nonadiabatic coupling. Two cases have been considered: (I) the avoided crossing between two potential surfaces, and (II) the spin-orbit interaction due to a 2P halogen atom. Comparisons are made between the results of the two-state model and the results of <i>ab initio</i> quantum chemical calculations.					
17. Key Words (Suggested by Author(s)) Atomic and molecular collisions Electronic transitions			18. Distribution Statement Unlimited STAR Category - 72		
19. Security Classif. (of this report) Unclassified		20. Security Classif. (of this page) Unclassified		21. No. of Pages 19	
				22. Price* \$3.25	

COMMENT ON THE RELATION BETWEEN THE NONADIABATIC COUPLING
AND THE COMPLEX INTERSECTION OF POTENTIAL ENERGY CURVES

Richard L. Jaffe

Ames Research Center

SUMMARY

Simple relations are discussed that provide a correspondence between the complex intersection of two potential surfaces and the nonadiabatic coupling matrix element between those surfaces. These are key quantities in semiclassical and quantum mechanical theories of collision-induced electronic transitions. Within the two-state approximation, the complex intersection is shown to be directly related to the location and magnitude of the peak in the nonadiabatic coupling. Two cases have been considered: (I) the avoided crossing between two potential surfaces, and (II) the spin-orbit interaction due to a 2P halogen atom. Comparisons are made between the results of the two-state model and the results of *ab initio* quantum chemical calculations.

1. Introduction

The first quantum mechanical calculations of collision-induced electronic transitions for model triatomic systems have been reported recently [1,2]. These studies considered electronic-to-vibrational [1] and electronic-to-rotational [2] energy transfer in nonreactive collisions of $^2P_{1/2}$ halogen atoms with hydrogen molecules. In addition, semiclassical calculations have been carried out for electronic transitions in $H^+ + D_2$ [3] and $H_2 + F(^2P_{1/2})$ [4] collisions based on the method developed by Miller and George [5]. Previously, quantum mechanical [6] and semiclassical [7] calculations had been reported for fine-structure transitions in atom-atom collisions. In the quantum mechanical studies, electronic transitions are induced by the nonadiabatic coupling matrix elements between the initial and final adiabatic electronic states (potential coupling). These coupling matrix elements can be calculated from the electronic wave functions or, to a good approximation, from the adiabatic electronic potential surfaces themselves [1,8]. For diatomic systems, adiabatic potential surfaces of the same symmetry and multiplicity do not intersect for real values of the nuclear coordinates, but complex-valued intersection points (branch points) do exist [9-13]. For larger systems, the surface of complex intersection always has a higher dimensionality than the surface of real intersection. The semiclassical theory makes use of the complex intersections to effect transitions between the potential surfaces. The collisions are simulated by classical trajectories which are analytically continued from one potential surface to the complex intersection and back to the second potential surface. The probability for making such a transition shows a roughly inverse dependence

on the distance from the real axis to the complex intersection point. The two methods are similar in that the factors which govern the magnitude of the transition probability are derived from the adiabatic potential surfaces involved. Davis and Pechukas [14] and Pechukas et al. [15] have shown that the semiclassical treatment is indeed a limiting case of the quantum mechanical theory. However, the problem of locating the complex intersection points must still be solved before semiclassical calculations of electronic transitions can be undertaken.

Ab initio molecular orbital calculations of potential energies at complex values of the nuclear coordinates have recently been performed for four systems. The location of the complex intersection points has been determined for the 3σ and 4σ states of HeH^{++} [10], the two lowest singlet states of H_3^+ [11] and the lowest $^2\Sigma$ and $^2\Pi$ states of collinear H_2F [12] and HF^+ [13]. In the first two systems, the potential surfaces for the two states exhibit avoided crossings for real-valued geometries, while, in the latter two systems, the potentials are parallel in the limit of separated $\text{H}^+ + \text{F}$ and $\text{H}_2 + \text{F}$, and are split by the spin-orbit coupling of the fluorine atom. There is no avoided crossing of the HF^+ potential curves which diverge as the internuclear separation is decreased. For the collinear H_2F system, the two states show (in addition to the asymptotic behavior discussed above) an avoided crossing at small HF distances. These studies have shown qualitative relationships for the location of the avoided crossing, the actual complex intersection point, and the extremum in the nonadiabatic coupling. For these systems, the complex intersection points were located by the analytical continuation of rational-fractions which had been numerically fit to the energy difference between the potential surfaces [16,17]. The real part of

the complex nuclear coordinate at an intersection point was found to be approximately equal to the value of that coordinate at both the extremum in the nonadiabatic coupling and the avoided crossing.

In this paper, the relationship between the complex intersection point and the nonadiabatic coupling is explored. It is shown that formal connections exist for special cases within the two-state approximation. The results for these cases are presented in Sections 2 and 3 and discussed in terms of the results of the complex-valued *ab initio* molecular orbital calculations. The above relationship can be used to help locate the complex intersection points for cases when the results of complex-valued molecular orbital calculations are not available. Section 4 contains some concluding remarks.

2. Case I: The avoided crossing

In the two-state model of an avoided crossing, the electronic Hamiltonian matrix is given by

$$\tilde{H} = \begin{pmatrix} H_{11}(\tilde{r}) & H_{12}(\tilde{r}) \\ H_{12}(\tilde{r}) & H_{22}(\tilde{r}) \end{pmatrix}, \quad (1)$$

where \tilde{r} is a vector that represents all the nuclear coordinates. The potential energies of states 1 and 2 are

$$E_j = \frac{H_{11} + H_{22}}{2} + (-1)^j \frac{\Delta E}{2}, \quad (2)$$

where

$$\Delta E = [(H_{22} - H_{11})^2 + 4H_{12}^2]^{1/2} \quad (3)$$

is the energy difference between the two adiabatic states. The nonadiabatic coupling between the states for coordinate α , in this approximation, is given by [8,12]

$$\chi_{12\alpha} = \frac{H_{12}}{\Delta E^2} \frac{\partial(H_{22} - H_{11})}{\partial \alpha} \quad (4)$$

In the following treatment, we assume that the electronic transition occurs only through motion along one generalized coordinate r and that the coupling matrix element H_{12} is independent of that coordinate. We also define the quantity f equal to $H_{22} - H_{11}$ and use primes to signify partial differentiation with respect to r .

Extrema in ΔE occur at those values of r for which

$$\Delta E' = ff'/\Delta E \quad , \quad (5)$$

that is, when $f = 0$ or $f' = 0$. Examination of $\Delta E''$ reveals that ΔE is *always* a minimum when $f = 0$. This case corresponds to the avoided intersection ($r = r_m$). Extrema in the nonadiabatic coupling are found by solving

$$\left[\frac{\partial \chi_{12r}}{\partial r} \right]_{r=r_c} = \frac{H_{12}f''}{\Delta E^2} - \frac{2H_{12}f[f']^2}{\Delta E^4} = 0 \quad (6)$$

From eq. (6) we conclude that the system will exhibit an extremum in the nonadiabatic coupling at a point of avoided intersection only if $f = f'' = 0$. To determine the condition for $r_m = \text{Re}r_0$, the real part of a point of complex intersection, we first expand $f(r)$ in a Taylor series about r_m :

$$f(r) = (r - r_m)f'(r_m) + \frac{(r - r_m)^2 f''(r_m)}{2} + \frac{(r - r_m)^3 f'''(r_m)}{6} + \dots \quad (7)$$

At a complex intersection point ($\Delta E = 0$) $f(r_0)$ must be pure imaginary and equal to $\pm i2H_{12}$. Since f is a real function of the complex variable r , $\text{Re } r_0 = r_m$ only if all even power terms in eq. (7) are zero (i.e., $f^{(2n)}(r_m) = 0$). This condition encompasses the one found above for $r_c = r_m$.

Two functional forms for f which exhibit the property $\text{Re } r_0 = r_m = r_c$ are

$$f = ar - b \quad (8)$$

and

$$f = A \sin(ar - b) \quad (9)$$

a , b , and A can be functions of any of the coordinates except r . Equation (8) has been used in the Landau-Zener treatment of electronic transitions [18].

In both cases,

$$r_m = b/a \quad \text{and} \quad \Delta E(r_m) = 2H_{12}.$$

The location of the complex intersection points for f given by eq. (8) are

$$r_0 = r_m \pm \frac{i\Delta E(r_m)}{a} \quad (10)$$

and the magnitude of the nonadiabatic coupling at r_c is $a/2\Delta E(r_m)$. Thus $|\chi_{12r}|$ has a single maximum of height $1/2 \text{Im } r_0$. This provides a demonstration of the behavior found in the semiclassical calculations; namely, the transition probability falls off inversely with the distance from the real-axis to the complex intersection point. When f is given by eq. (9), complex intersection points are given by

$$r_0 = r_m \pm \frac{i}{a} \sinh^{-1} \left[\frac{\Delta E(r_m)}{A} \right] \quad (11)$$

and

$$\chi_{12r}(r_c) = \frac{Aa}{2\Delta E(r_m)} \quad (12)$$

while $|\chi_{12r}|$ is not simply proportional to $2/\text{Im}r_0$, it still decreases with increasing $\text{Im}r_0$. For both cases, the strength of the transition is proportional to the slope of f at $r = r_m$.

The half width, W , of the peak in χ_{12r} provides a measure of the degree to which the electronic transition is localized around r_c . W is equal to $r^+ - r^-$, where r^\pm are obtained by inversion of eq. (4) with $\chi_{12r} = \chi_{12r}(r_c)/2$. For f given by eq. (8):

$$r^\pm = r_m \pm \Delta E(r_m)/a, \quad (13)$$

so the half width of the peak in the nonadiabatic coupling matrix element is simply $2\Delta E(r_m)/a = [\chi_{12r}(r_m)]^{-1}$. Thus, the stronger the coupling, the more localized the transition.

The reliability of this model can be tested by comparison with the *ab initio* data for HeH^{++} and H_3^+ . For HeH^{++} [10], the energies of the 3σ and 4σ states ($E_{3\sigma}$ and $E_{4\sigma}$) were determined from the third and fourth eigenvalues of a 16×16 electronic Hamiltonian matrix as a function of r , the internuclear separation. The avoided crossing was located at $r_m = 3.6440$ bohr, the value of r that minimized $\Delta E = E_{4\sigma} - E_{3\sigma}$. The electronic transition in $\text{H}_2 + \text{H}^+ \rightarrow \text{H}_2^+ + \text{H}$ collisions occurs between the first and second singlet potential surfaces of H_3^+ . In this system, for collinear or isosceles triangle geometries, there are two nuclear coordinates,* r and R , and the loci of avoided crossings and complex

* For collinear geometries, r and R are the distances between the central atom and the two outer atoms with $r < R$. For isosceles triangle geometries, r and R are the base and altitude of the triangle, respectively. In the first and second singlet states of H_3^+ , r corresponds to the vibrational coordinate for H_2 and H_2^+ , respectively, and R corresponds to the translational coordinate.

intersection points lie on curves of (r, R) through configuration space.

Ab initio calculations were performed to locate r_m and r_0 for fixed values of R [11]. It was found that r_m is roughly unchanged for values of $R > 6$ bohr, indicating that the electronic transition is effected through vibrational motion during the collision.

For these two systems, α can be obtained from the slope of a linear fit of r versus $f = \pm\{[\Delta E(r)]^2 - [\Delta E(r_m)]^2\}^{1/2}$ ** and $\text{Im}r_0$ is predicted from eq. (10). The results are shown in table 1 for four sets of data from the *ab initio* calculations. For small H_{12} , the errors in the results of the model are less than 1/2% when compared with the *ab initio* data, as can be seen for the HeH^{++} and H_3^+ $R = 9$ bohr results in table 1. However, for larger H_{12} , the model breaks down. $f(r)$ is still nearly linear and $\text{Im}r_0$ can be predicted to within 90% of the true value, but the model cannot account for the shift in $\text{Re}r_0$ away from r_m . The fitting of $f(r)$ to a rational-fraction in r [17] improves the two-state model. However, r_0 and r_c could no longer be determined analytically and the relation $r_m = r_c = \text{Re } r_0$ would no longer hold.

Thus, this simplified model of an avoided crossing is quite accurate when applied to systems with weak coupling (H_{12}) for which a definite relation exists between the factors that influence the quantum and semiclassical transition probabilities. This implies that the electronic transition is localized at $r = r_m$ and the complex intersection points can be located with the use of the real-valued potential energy surfaces. However, for stronger coupling, the correspondence between the two methods no longer holds, and

** f is positive for $r < r_m$ and negative for $r > r_m$.

one must know the potential energies at complex values of the nuclear coordinates to carry out semiclassical calculations of electronic transitions.

3. Case II: Spin-orbit coupling and fine-structure transitions

The spin-orbit interaction for atom-atom and collinear atom-diatom collisions involving 2P_u halogen atoms can often be treated within the framework of a two-state approximation [7,12,19,20]. In these systems, the nonrelativistic description of the halogen atom has a degenerate ground state which splits into $^2P_{3/2}$ and $^2P_{1/2}$ components upon the inclusion of spin-orbit coupling. The potential curves for an $A + X$ collision (A is any nondegenerate atomic or diatomic species and X is a halogen atom) are parallel at large $A-X$ separations with an energy difference equal to λ , the halogen atom spin orbit splitting. These asymptotes correspond to $A + X (^2P_{3/2})$ and $A + X (^2P_{1/2})$. The potential curves are subject to the same constraints regarding real and complex intersections as in the case of an avoided crossing.

Within this approximation, the complete Hamiltonian matrix is given by eq. (1) with $H_{11} = V_{\Pi} + \lambda/3$, $H_{22} = V_{\Sigma}$, and $H_{12} = (2)^{1/2}(\lambda/3)$. V_{Π} and V_{Σ} are the nonrelativistic potential energy surfaces for the lowest Π and Σ states of the system [12]. For this case, eq. (3) becomes

$$\Delta E = [(\Delta V + \lambda/3)^2 + 8\lambda^2/9]^{1/2}, \quad (14)$$

where $\Delta V = V_{\Pi} - V_{\Sigma}$. At the asymptotic limit, $\Delta V = 0$ and ΔE equals λ .

The complex intersections occur when $\Delta V = \Delta V_0$,

$$\Delta V_0 = \lambda \exp [\pm i \cos^{-1}(-1/3)]. \quad (15)$$

If $\Delta V + (\lambda/3)$ equals zero, there will still be an avoided crossing with its associated complex intersection points as in case I. However, additional complex intersection points are caused by the asymptotic behavior of ΔV . Since ΔV can be qualitatively represented by functions like x^{-n} or e^{-x} , the relations found for case I are not applicable to the spin-orbit case.

Preston, Sloane, and Miller [7] have fit ΔV to an exponential function in the internuclear separation, r ,

$$\Delta V(r) = A \exp(-\alpha r) \quad (16)$$

for the Xe + F system in which V_{Σ} is the ground state. We use this form in the following treatment of fine-structure transitions. For collinear $H_2 + F$, r represents the HF separation with A and α taken to be functions of the HH bond length. Using eqs. (15) and (16), the complex intersection occurs when

$$r_0 = \frac{1}{\alpha} \left[\ln \left(\frac{A}{\lambda} \right) \pm i \cos^{-1} \left(-\frac{1}{3} \right) \right]. \quad (17)$$

In considering the HF^+ system in which $V_{\Pi} < V_{\Sigma}$ for all r , $|\Delta V(r)|$ must be fit to the exponential in eq. (16) and r_0 is given by

$$r_0 = \frac{1}{\alpha} \left[\ln \left(\frac{A}{\lambda} \right) \pm i \cos^{-1} \left(+\frac{1}{3} \right) \right]. \quad (17')$$

Thus, $\text{Im } r_0$ depends only on the difference in shape between the nonrelativistic potential curves while $\text{Re } r_0$ depends on both the strength of the spin-orbit coupling and the nature of ΔV . The faster ΔV goes to zero with increasing r , the greater the electronic transition probability, since the complex intersection is located closer to the real axis.

The nonadiabatic coupling, as given by eq. (4), has extrema at the values of r for which

$$\left[\frac{\partial \chi_{12r}}{\partial r} \right]_{r=r_c} = - \frac{\sqrt{2} \lambda \alpha^2 \Delta V(r_c)}{3 \Delta E(r_c)^4} \left[\Delta V(r_c)^2 - \lambda^2 \right] = 0 \quad (18)$$

These occur for $r = \pm \infty$, where $\chi_{12r} = 0$, and when $|\Delta V| = \lambda$.

At the latter point, $r = r_c$, which is given by

$$r_c = \frac{1}{\alpha} \ln \left(\frac{A}{\lambda} \right) = \text{Re } r_0 \quad (19)$$

Thus, in this case, as in case I, the location of the extremum in the nonadiabatic coupling coincides with the real part of the complex crossing point. In addition,

$$\chi_{12r}(r_c) = - \frac{\sqrt{2} \alpha}{8} = - \frac{\sqrt{2} \cos^{-1} \left(- \frac{1}{3} \right)}{8 \text{Im } r_0}, \quad V_{\text{II}} > V_{\Sigma} \quad (20)$$

or

$$\chi_{12r}(r_c) = - \frac{\sqrt{2} \alpha}{4} = - \frac{\sqrt{2} \cos^{-1} \left(+ \frac{1}{3} \right)}{8 \text{Im } r_0}, \quad V_{\Sigma} > V_{\text{II}} \quad (20')$$

and

$$W = \frac{1}{\alpha} \ln \left(\frac{7 + 2\sqrt{10}}{7 - 2\sqrt{10}} \right), \quad V_{\text{II}} > V_{\Sigma} \quad (21)$$

or

$$W = \frac{1}{\alpha} \ln 9, \quad V_{\Sigma} > V_{\text{II}} \quad (21')$$

These results, which are summarized in table 2, are also similar to the relations found for case I. However, $\text{Im } r_0$, $\chi_{12}(r_c)$, and W do not depend on the strength of the spin-orbit coupling.

The available *ab initio* data can be used to test this model as was done for case I. Calculations of V_{Σ} and V_{II} as a function of r , the H-F

separation, have been performed for H_2F [12] in collinear geometries with the H-H bond fixed at 1.4 bohr (the equilibrium separation in H_2) and HF^+ [13,20]. These calculations incorporated the spin-orbit interaction within the framework of the two-state model discussed above. In the former system, V_Σ is the ground-state surface at small r , but a shallow well in the Π -state causes $V_\Pi \leq V_\Sigma$ for r greater than 4.7 bohr. Thus, ΔV exhibits a minimum of -2.8×10^{-4} hartrees at 5.4 bohr and cannot be represented by eq. (16). However, r_0 can be predicted from r_c and $\chi_{12r}(r_c)$ by using eqs. (17) and (20). The resulting complex intersection point, $2.023 \pm 0.633i$ bohr, is in fair agreement with the *ab initio* value, $r_0 = 2.041 \pm 0.429i$. For HF^+ , $V_\Pi \leq V_\Sigma$ for all r , and ΔV is better represented by eq. (16). However, a plot of $\ln \Delta V$ versus r shows considerable curvature [13,20]. The data from the *ab initio* MO calculations of ΔV are in good agreement for $r \leq 5$, but the results of Jaffe et al. [13] fall off less steeply than do those of ref. [20] at larger r . The calculated values of r_0 and $\chi_{12r}(r_c)$ for various fits of these data to eq. (16) are presented in table 3. It can be seen that good values for $\text{Im } r_0$ and $\chi_{12r}(r_c)$ are obtained from the fit to the $r \geq 6$ data and that no fit reproduces $\text{Re } r_0$ and r_c accurately. However, use of the *ab initio* data for r_c and $\chi_{12r}(r_c)$ leads to an accurate prediction of the location of the complex intersection point, even though the actual data points cannot be accurately fit to eq. (16).

For HF^+ , it has been noted [7] that ΔV could be better represented by

$$\Delta V = A \exp[-\alpha r + \beta r^2] \quad . \quad (22)$$

In this case, eq. (18) becomes a transcendental equation in r and an analytic solution for r_c is not possible. Numerical determinations of the

extrema of χ_{12r} have been carried out for various values of A , α , and β .

The location of the complex intersections have been shown to be [7,13]

$$r_0 = \left\{ \alpha - \left(\alpha^2 - 4\beta \left[\ln \left(\frac{A}{\lambda} \right) \pm i \cos^{-1} \left(+ \frac{1}{3} \right) \right] \right)^{1/2} \right\} / 2\beta . \quad (23)$$

The relations between r_0 and χ_{12r} are in very close agreement with the above case for $\beta < 0.03 \alpha$, but only at $\beta = 0$ is r_c exactly equal to $\text{Re } r_0$. In addition, an empirical relation has been found between $\chi_{12r}(r_c)$ and $\text{Im } r_0$

$$\left| \frac{\chi_{12r}(r_c)}{\text{Im } r_0} \right| = \frac{\sqrt{2}}{4 \cos^{-1} \left(+ \frac{1}{3} \right)} \left[\alpha^2 - 4\beta \ln \left(\frac{A}{\lambda} \right) \right] , \quad \beta \leq \alpha^2 / 4 \ln \left(\frac{A}{\lambda} \right) . \quad (24)$$

In ref. [13], it is reported that r_0 is quite sensitive to which data points are used to determine A , α , and β by a least-squares fitting procedure. The empirical relation given by eq. (21) suggests that the *best* value of $\text{Im } r_0$ is that obtained from the parameters for which the fitted and *ab initio* data for $\chi_{12r}(r_c)$ are in closest agreement, provided, of course, that $\beta \leq \alpha^2 / 4 \ln (A/\lambda)$. This criterion provides a means of selecting the optimum parameters in eq. (22) when an *ab initio* calculation of the complex intersection is not available. Examination of the detailed results of the least-squares fits used in ref. [13] confirms the validity of this procedure. However, r_0 can only be located to within $(0.03 + 0.01i)$ bohr by this method.

4. Conclusions

It has been shown that simple relations exist among the quantities which govern the electronic transition probability in quantum and semiclassical scattering theory for two special cases. For an avoided crossing, these

relations hold when the coupling between the electronic states (H_{12}) is small and the transition is localized at the avoided intersection. This condition should encompass most cases with large transition probabilities. In semiclassical calculations, the complex intersection points can be located with the use of the slope of a linear fit of H_{11} - H_{22} . In this way, semiclassical calculations can be carried out using only real-valued potential energy surfaces as input.

For the spin-orbit case, it has been shown that the nonadiabatic coupling and location of the complex intersection points are very sensitive to ΔV , the difference between the nonrelativistic potential surfaces. Simple relations exist for these quantities in systems with relatively short-range interactions (large α 's and small or negative β 's in eqs. (16) and (22)). Again, this provides a method to help locate the complex intersection points needed for semiclassical calculations of electronic transitions when only real-valued potential energy surfaces are available. However, in this case more caution is needed as the location of complex intersection points is very sensitive to the functional form used to fit the ΔV versus r data

References

- [1] I. H. Zimmerman and T. F. George, J. Chem. Phys. 61 (1974) 2468;
I. H. Zimmerman and T. F. George, Chem. Phys. 7 (1975) 323.
- [2] F. Rebertus and W. A. Lester, J. Chem. Phys. 64 (1976) 4223.
- [3] Y. W. Lin, T. F. George and K. Morokuma, Chem. Phys. Letters 22
(1973) 547; Y. W. Lin, T. F. George and K. Morokuma, Chem. Phys. Letters 30
(1975) 49.

- [4] A. Komornicki, T. F. George and K. Morokuma, J. Chem. Phys. 65 (1976) 48.
- [5] W. H. Miller and T. F. George, J. Chem. Phys. 56 (1972) 5637.
- [6] F. H. Meis, Phys. Rev. A7 (1973) 942, 957.
- [7] R. K. Preston, C. Sloane and W. H. Miller, J. Chem. Phys. 60 (1974) 4961.
- [8] J. C. Tully, J. Chem. Phys. 59 (1973) 5122.
- [9] T. F. George, K. Morokuma and Y. W. Lin, Chem. Phys. Letters 30 (1975) 54.
- [10] K. Morokuma and T. F. George, J. Chem. Phys. 59 (1973) 1959.
- [11] R. L. Jaffe, K. Morokuma and T. F. George, J. Chem. Phys. 61 (1974) 4717.
- [12] R. L. Jaffe, K. Morokuma and T. F. George, J. Chem. Phys. 63 (1975) 3417.
- [13] R. L. Jaffe, A. D. Isaacson, J. R. Laing, K. Morokuma and T. F. George, Theoret. Chim. Acta 40 (1975) 189.
- [14] J. P. Davis and P. Pechukas, J. Chem. Phys. 64 (1976) 3129.
- [15] P. Pechukas, T. F. George, K. Morokuma, F. J. McLafferty and J. R. Laing, J. Chem. Phys. 64 (1976) 1099.
- [16] T. F. George and K. Morokuma, Chem. Phys. 2 (1973) 129.
- [17] R. L. Jaffe, T. F. George and K. Morokuma, Mol. Phys. 28 (1974) 1489.
- [18] L. D. Landau, Physik Z. Sowjetunion U.R.S.S. 2 (1932) 46; C. Zener, Proc. R. Soc. A 137 (1932) 696.
- [19] D. G. Truhlar, J. Chem. Phys. 56 (1972) 3189; J. T. Muckerman and M. D. Newton, *ibid.* 56 (1972) 3191.
- [20] P. Julienne, M. Krauss and A. C. Wahl, Chem. Phys. Letters 11 (1971) 16.

Comparison of predictions from the two-state model of avoided crossings
with complex-valued *ab initio* MO data

Case	r_m (bohr)	$\Delta E(r_m)$ (hartree)	a^a (hartree bohr ⁻¹)	r_0 (bohr)	r_0 predicted ^{b)} (bohr)	quality ^{c)} of fit
HeH ^{++d)}	3.6440	0.00294	-0.0784	$3.6440 \pm 0.0375i$	$3.6446 \pm 0.0375i$	1.48
H ₃ ⁺ collinear ^{e)}	2.447	0.00117	-0.0542	$2.4482 \pm 0.0218i$	$2.449 \pm 0.0218i$	1.92
(R = 9 bohr)						
H ₃ ⁺ collinear ^{e)}	2.448	0.01683	-0.0527	$2.3926 \pm 0.2959i$	$2.446 \pm 0.3193i$	5.39
(R = 6 bohr)						
H ₃ ⁺ triangular ^{e)}	2.468	0.02621	-0.0515	$2.3464 \pm 0.4439i$	$2.468 \pm 0.5090i$	4.67
(R = 6 bohr)						

a) Determined by linear least squares fit of $f(r)$.

b) r_0 predicted = $r_m \pm i\Delta E(r_m)/a$.

c) Defined as $100 \times \left[\frac{\sum_i (f_i^{\text{fit}} - f_i)^2}{\sum_i f_i^2} \right]^{1/2}$

d) Data from ref. [10].

e) Data from ref. [11] for $[5s, 2p] \rightarrow (3s, 1p)$ basis set.

Table 2

Summary of interrelations for case II

$$W = 2.98199/\alpha, \quad V_{\Pi} > V_{\Sigma}$$

$$W = 2.19722/\alpha, \quad V_{\Sigma} > V_{\Pi}$$

$$|\chi_{12r}(r_c)| = 0.17678/\alpha, \quad V_{\Pi} > V_{\Sigma}$$

$$|\chi_{12r}(r_c)| = 0.35355/\alpha, \quad V_{\Sigma} > V_{\Pi}$$

$$|\chi_{12r}(r_c)| = 0.33776/\text{Im } r_0, \quad V_{\Pi} > V_{\Sigma}$$

$$|\chi_{12r}(r_c)| = 0.43521/\text{Im } r_0, \quad V_{\Pi} > V_{\Sigma}$$

$$\text{Im } r_0 = \pm 1.91063/\alpha, \quad V_{\Pi} > V_{\Sigma}$$

$$\text{Im } r_0 = \pm 1.23096/\alpha, \quad V_{\Sigma} > V_{\Pi}$$

Table 3

Comparison of the model with *ab initio* MO data for HF^+

Case ^{a)}	α (bohr ⁻¹)	A (hartree)	r_c (bohr)	$\chi_{12r}(r_c)$ (bohr ⁻¹)	r_0 (bohr)
fit to $r \leq 5$ data	0.91	0.76	6.619	0.322	6.619 ± 1.3531
fit to $r \geq 6$ data	0.39	0.048	8.305	0.138	8.305 ± 3.15611
fit to all data	0.62	0.235	7.822	0.219	7.822 ± 1.9851
<i>ab initio</i> results	-	-	7.4	0.141	7.495 ± 3.0091
(i) predicted from $r_c, \chi_{12r}(r_c)$	0.399	0.035	-	-	7.4 ± 3.0871
(ii) predicted from r_0	0.409	0.039	7.495	0.145	---

a) *ab initio* data taken from ref. [13].